

# Cryogenic magnetocaloric effect in the Fe<sub>17</sub> molecular nanomagnet

Ian A. Gass<sup>a</sup>, Euan K. Brechin<sup>a</sup>, Marco Evangelisti<sup>b,\*</sup>

<sup>a</sup> *School of Chemistry, The University of Edinburgh, West Mains Road, EH9 3JJ*

*Edinburgh, United Kingdom*

<sup>b</sup> *Instituto de Ciencia de Materiales de Aragón, CSIC-Universidad de Zaragoza,*

*Departamento de Física de la Materia Condensada, 50009 Zaragoza, Spain*

## Abstract

We study the magnetothermal properties of magnetically isotropic high-spin molecular nanomagnets containing 17 Fe<sup>3+</sup> ions per molecule linked via oxide and hydroxide ions, packed in a crystallographic cubic symmetry. Low-temperature magnetization and heat capacity experiments reveal that each molecular unit carries a net spin ground state as large as  $S = 35/2$  and a magnetic anisotropy as small as  $D = -0.023$  K, while no magnetic order, purely driven by dipolar interactions, is to be expected down to very-low temperatures. These characteristics suggest that the Fe<sub>17</sub> molecular nanomagnet can potentially be employed as a sub-Kelvin magnetic refrigerant.

**Keywords:** Iron; Magnetite; Magnetocaloric effect; Magnetic refrigeration; Cryogenics

\* Corresponding author. WWW address: <http://molchip.unizar.es/>

*Footnote:* Dedicated to Alfred Werner on the 100<sup>th</sup> Anniversary of his Nobel prize in Chemistry in 1913.

## 1. Introduction

The topic of magnetic refrigeration constitutes one of the most promising applications envisioned for molecule-based materials, specifically molecular nanomagnets [1]. The refrigeration process is based on the magnetocaloric effect (MCE), i.e. the change of the magnetic entropy and related adiabatic temperature upon the change of an applied magnetic field. All magnetic materials intrinsically show MCE, although the intensity of the effect depends on the properties of each material. Besides the fundamental interest on related magnetic and magnetothermal properties of novel materials, MCE is of great technological importance since it can be used for cooling applications [2] according to a process known as adiabatic demagnetization [3]. This technique is particularly promising for refrigeration at very low temperature, beyond the reach of liquid helium-4, providing, e.g., a valid alternative to the use of helium-3 which is quickly becoming rare and expensive. However, a sine-qua-non condition for achieving this target resides in the absence of a magnetic phase transition down to such low temperatures [4]. While the MCE is maximized at the critical temperature ( $T_C$ ) of a magnetically ordered region, it also steeply falls to near zero values below  $T_C$ , limiting indeed the lowest temperature which can be attained in an adiabatic demagnetization.

In molecular nanomagnets, a net magnetic moment (spin) can be defined for each individual molecule as a result of dominant intramolecular magnetic interactions. If one targets a large MCE, it is easy to demonstrate that the molecular nanomagnet should have a high spin state, in addition to a minimal anisotropy [5-7]. This is because: *(i)* the higher the spin value the larger the density of spin levels and thus the larger the magnetic entropy content; *(ii)* a negligible anisotropy permits easy polarization of the net molecular spins in magnetic fields of weak or moderate strength. These two pre-

requisites therefore dictate the synthetic strategy for obtaining the molecular nanomagnets that can be potentially exploited for magnetic refrigeration at the molecular level. The synthesis of the  $\text{Fe}_{17}$  molecular nanomagnet, containing 17  $\text{Fe}^{3+}$  ions per molecule linked via oxygen atoms derived from oxide and hydroxide ions (Fig. 1) was reported by some of us [8]. Magnetic studies on this and related molecules belonging to the same family, show that the spin ground state is as large as  $S = 35/2$ , whilst the anisotropy  $D$  is uniaxial, although extremely small with typical values of the order of  $10^{-2}$  K [8-11]. Further interest stems from the ability of finely controlling the mechanism of long-range magnetic order, driven by dipolar interactions, in crystals of  $\text{Fe}_{17}$  molecular nanomagnets [9]. This is made possible since the  $\text{Fe}_{17}$  molecular nanomagnets can be chemically arranged in different packing crystals without affecting the individual molecules, i.e., keeping the high-spin ground state and magnetic anisotropy unaltered. It seems therefore logical to investigate further the title compound in order to ascertain whether this material represents the excellent candidate for magnetic refrigeration as its properties seem to promise. Herein, we present our first MCE study of the  $\text{Fe}_{17}$  molecular nanomagnet. We focus on the crystallographic cubic symmetry, since this is known to minimize the dipolar energy, pushing  $T_C$  down to temperatures below  $\sim 0.3$  K [9], in marked contrast with, e.g., the crystallographic trigonal symmetry for which  $T_C \cong 1.1$  K [11].

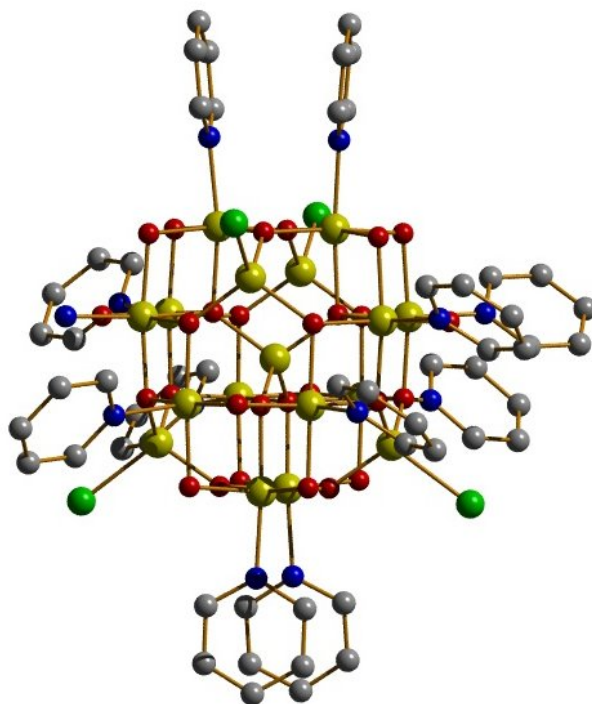


Fig. 1. The molecular structure of  $[\text{Fe}_{17}\text{O}_{16}(\text{OH})_{12}(\text{pyr})_{12}\text{Br}_4]\text{Br}_3$  (**1**); colour scheme, Fe = yellow, O = red, N = blue; Br = green, C = grey. (For interpretation of the references in colour in this figure legend, the reader is referred to the web version of this article.)

## 2. Experimental methods

In order to prepare the samples, the synthesis is simple – dissolution of anhydrous  $\text{FeBr}_3$  in a coordinating base, e.g., pyridine (pyr) with stirring leads to a dark red solution which, after approximately one hour, is then filtered and allowed to evaporate. Dark red crystals  $[\text{Fe}_{17}\text{O}_{16}(\text{OH})_{12}(\text{pyr})_{12}\text{Br}_4]\text{Br}_3$  (hereafter denoted as **1**) form within three days. The yield can be improved by adding a co-solvent of crystallization such as isopropylalcohol, resulting in a crystallographic arrangement of  $\text{Fe}_{17}$  molecules with the cubic space group symmetry  $Pa-3$  with  $a = b = c = 29.285(3)$  Å [9]. The yield is approximately 30%. Complex **1** contains a central tetrahedral  $\text{Fe}^{3+}$  ion linked via  $\mu_4$ -oxo

bridges to 12 outer octahedral  $\text{Fe}^{3+}$  ions – forming a truncated tetrahedron (Fig. 1). These ions are linked to each other via a combination of  $\mu_3$ - and  $\mu_4$ -oxides, and  $\mu_2$ -hydroxide ligands. The hexagonal faces of the truncated tetrahedron are capped by four further  $\text{Fe}^{3+}$  ions each linked via three  $\mu_3$ -oxo ligands. The inner  $\text{Fe}^{3+}$  ion and the four outer  $\text{Fe}^{3+}$  ions sit in the tetrahedral sites of the ‘lattice’, with the others occupying the octahedral sites. The four bromide ions cap the outer tetrahedral  $\text{Fe}^{3+}$  ions with the pyr molecules capping the octahedral  $\text{Fe}^{3+}$  ions. The Fe–O–Fe bridges fall into two clear categories [8]: those that connect the tetrahedral  $\text{Fe}^{3+}$  ions to the octahedral  $\text{Fe}^{3+}$  ions are all characterized by angles in the range  $\sim 121\text{--}127^\circ$ , whilst those that bridge solely between octahedral  $\text{Fe}^{3+}$  ions are characterized by angles in the range  $\sim 93\text{--}100^\circ$ . The oxidation states of both Fe and O centres were confirmed by bond length and charge balance considerations, and bond-valence-sum calculations [8].

Measurements of magnetization down to 2 K and heat capacity down to  $\sim 0.3$  K were carried out for the  $0 < B_0 < 7$  T magnetic field range. Since all experiments were performed on powder samples, the calculated fits were obtained taking into account spin random orientations.

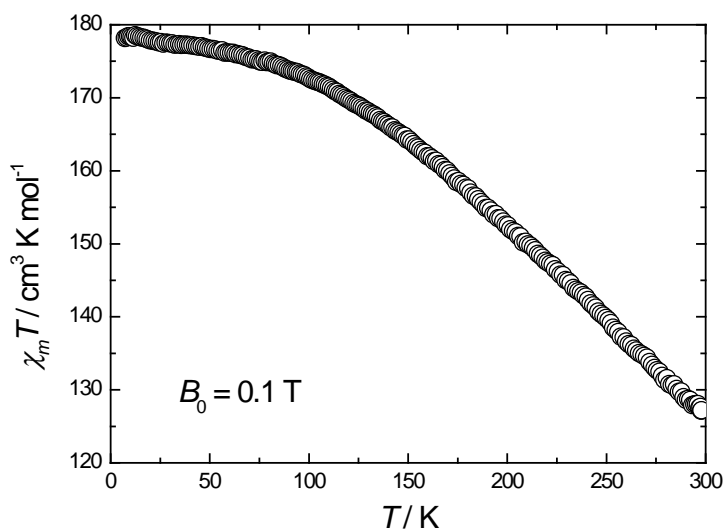


Fig. 2. Experimental temperature ( $T$ ) dependence of the  $\chi_M T$  product, where  $\chi_M$  is the molar susceptibility, collected for an applied field  $B_0 = 0.1$  T.

## 2. Magnetic and magnetothermal properties

Variable-temperature magnetic susceptibility data were collected on **1** in the temperature range 300 – 5 K for an applied field of 0.1 T (Fig. 2). The room-temperature  $\chi_M T$  value of approximately  $120 \text{ cm}^3 \text{ K mol}^{-1}$  rises constantly as temperature is decreased to a maximum value of approximately  $180 \text{ cm}^3 \text{ K mol}^{-1}$  at 5 K. The spin-only ( $g = 2.0$ ) value for an uncoupled  $[\text{Fe}^{3+}_{17}]$  unit is approximately  $74 \text{ cm}^3 \text{ K mol}^{-1}$ . This behaviour is indicative of dominant antiferromagnetic exchange between the metal centres with the low-temperature (5 K) maximum indicating an  $S \approx 35/2$  spin ground state.

In order to determine the spin ground state for **1**, magnetisation data were collected in the ranges 0 – 7 T and 2 – 20 K and these are plotted in Figure 3. It can be seen that

saturation occurs at a value of approximately  $36 \mu_B$ , in agreement with the spin ground state estimated above on basis of the susceptibility experiment. For a precise determination, we fitted the magnetization data by a matrix-diagonalization method to a model that includes the Zeeman term and axial zero-field splitting. Although smaller anisotropy components could be present, the data do not justify a more sophisticated fitting. The corresponding Hamiltonian is given by:

$$H = DS_z^2 + g\mu_B \vec{B} \cdot \vec{S} \quad (1)$$

The best fit gave  $S = 35/2$ ,  $g = 2.06$ , and  $D = -0.023$  K. The ground state can be rationalized by assuming an antiferromagnetic interaction between the tetrahedral and octahedral  $\text{Fe}^{3+}$  sites – consistent with the two distinct categories of Fe-O-Fe bridging angles present in the complex [8].

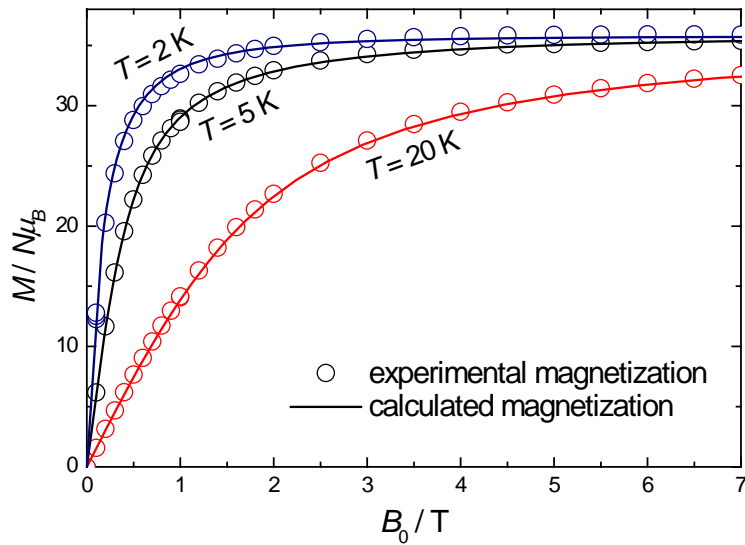


Fig. 3. Isothermal molecular magnetization of **1** collected for  $T = 2, 5$  and  $20$  K. Solid lines are the results of the fit (see text), yielding net molecular spin  $S = 35/2$  and axial  $D = -0.023$  K.

The magnetothermal properties of **1** were studied by means of heat capacity  $C(T, B_0)$  experiments. Figure 4 shows the collected  $C(T, B_0)$  data as a function of temperature for several applied fields. Because of the small anisotropy ( $D = -0.023$  K), it is expected that the magnetic contribution to  $C(T, B_0)$  for  $B_0 \geq 1$  T is due to Schottky-like Zeeman splitting of the otherwise nearly degenerate energy spin states [12]. Indeed, the calculated Schottky curves (solid lines in Fig. 4) arising from the field-split levels, and assuming  $g = 2.0$ , account very well for the experimental data. From the zero-field heat capacity, we further notice that no onset of phase transition exists, at least down to the minimum temperature of  $\sim 0.3$  K, suggesting that the  $\text{Fe}_{17}$  molecules are magnetically isolated from each other, as also suggested by the large intermolecular distances [8]. Not even the unavoidable magnetic dipolar intermolecular interactions play any role in this temperature range, since the cubic crystal symmetry essentially cancels them out [9].

We estimate the lattice contribution (dashed line in Fig. 4) by fitting to a model given by the sum of a Debye term for the acoustic low-energy phonon modes plus an Einstein term that likely arises from intramolecular vibrational modes. The best fit provides the values of  $\theta_D \cong 23$  K and  $\theta_E \cong 42$  K for the Debye and Einstein temperatures, respectively. The so-obtained lattice contribution allows us to estimate the magnetic entropy as a function of temperature by using the relation:

$$S(T)/R = \int_0^T C_m(T)/(RT) \cdot dT, \quad (2)$$

where  $C_m(T)$  is the magnetic contribution obtained from  $C(T)$  after subtraction of the respective lattice contribution. The so-obtained  $S(T)$  is depicted in the inset of Figure 4



for several applied field changes. It can be seen that total entropy content tends to the expected value for a fully occupied spin state  $S = 35/2$ , i.e.  $R\ln(2S+1) \cong 3.6$ .

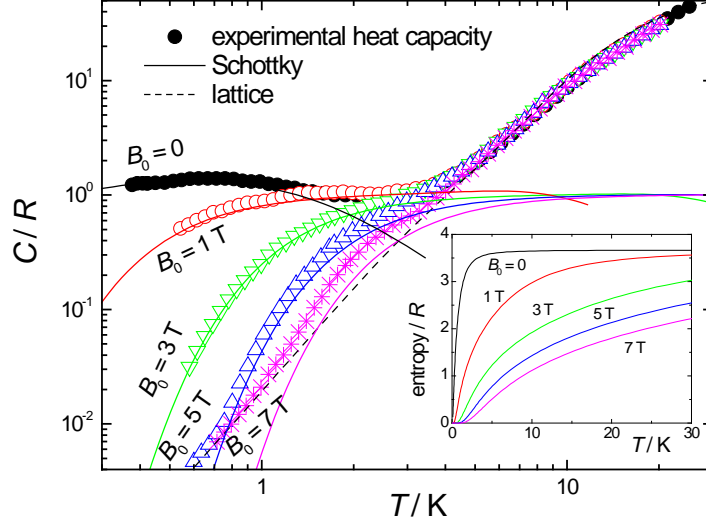


Fig. 4. Temperature-dependence of the heat capacity of **1** normalized to the gas constant  $R$  for several applied fields, as labelled. Solid curves are explained in the main text. Inset: Temperature-dependence of the magnetic entropy normalized to the gas constant  $R$  for several applied fields, as obtained from the heat capacity data.

We next evaluate the MCE, specifically the magnetic entropy change  $\Delta S_m(T, B_0)$ , which can straightforwardly be estimated from the entropy curves plotted in the inset of Figure 4. Figure 5 shows that **1** has the maximum  $-\Delta S_m(T, B_0)$  of  $8.9 \text{ J kg}^{-1} \text{ K}^{-1}$  at  $T = 2.7 \text{ K}$  for the applied-field change  $\Delta B_0 = (7 - 0) \text{ T}$ . This value for the entropy change is equivalent to  $\sim 3.3 R$ , which is not too distant from the total entropy of the system associated with the spin ground state  $S = 35/2$ , i.e.,  $R\ln(2S+1) = 3.6 R$ , to achieve which an applied field change  $\Delta B_0$  of about  $7 \cdot 3.6 / 3.3 \cong 7.6 \text{ T}$  should be needed. The very large value of the

spin ground state has also a further result which is that of promoting relatively large applied-field splittings of the  $S = 35/2$  multiplet. This implies that the entropy change maintains its relatively large value over a remarkably wide temperature range, for instance for  $\Delta B_0 = (7 - 0)$  T,  $-\Delta S_m$  reaches the half value of its maximum only at  $T \cong 24.5$  K, i.e. a temperature of more than 9 times larger than that at which the maximum is observed (Figure 5).

We finally notice that the MCE of **1** has moderate values if compared with that reported in the recent literature for several gadolinium-based molecular nanomagnets [13], for instance  $-\Delta S_m(T, B_0)$  of  $[\{\text{Gd}(\text{OAc})_3(\text{H}_2\text{O})_2\}_2] \cdot 4\text{H}_2\text{O}$  reaches values over  $40 \text{ J kg}^{-1} \text{ K}^{-1}$  at  $T = 1.8$  K and  $\Delta B_0 = (7 - 0)$  T [13d]. However, we also point out that, in spite of the large MCE of these molecules, the minimum temperature that they can reach in an adiabatic demagnetization process is limited by their long-range magnetic ordering temperature. A solution that has been successfully employed for screening all interactions between molecules consists in encapsulating each of them by closed frameworks, which act as capping ligands [4]. The inherent downside of this approach is that the so-added framework, being non-magnetic and hence passively participating in the MCE, ultimately lowers  $-\Delta S_m(T, B_0)$ , e.g. reaching a maximum of only  $1.9 \text{ J kg}^{-1} \text{ K}^{-1}$  at  $T = 1.3$  K and  $\Delta B_0 = (7 - 0)$  T in  $\text{GdW}_{30}$  [4]. An alternative solution for an effective intermolecular screening could be suggested by the herein investigated  $\text{Fe}_{17}$  molecular nanomagnets. Indeed, rather than increasing the molecular mass, one can target the packing of the molecules in crystallographic symmetries that minimize the dipolar energy, such as in **1** [9].

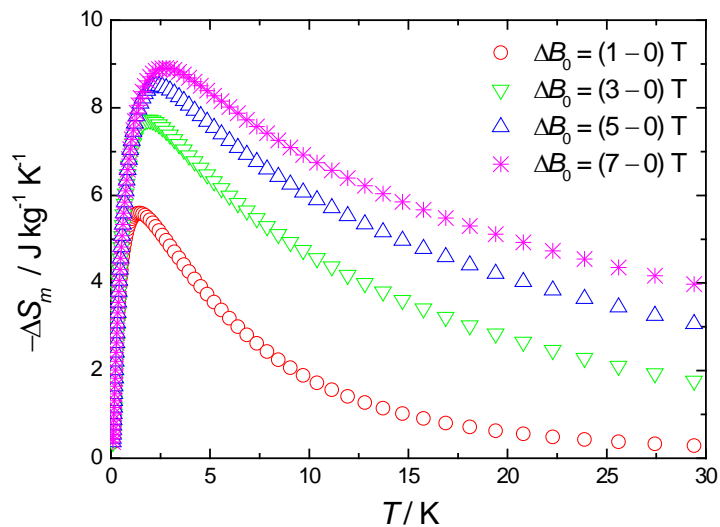


Fig. 5. Temperature-dependence of the magnetic entropy change  $\Delta S_m$  of **1**, as obtained from heat capacity data (Fig. 4) for the indicated applied-field changes  $\Delta B_0$ .

#### 4. Conclusions

In conclusion, a polynuclear  $\text{Fe}^{3+}$ -based molecular complex has been studied for its potential application in magnetic refrigeration for very low temperatures. The combination of high spin and low magnetic anisotropy was the main attraction of this material for the determination of its magnetocaloric effect, which we have evaluated from heat capacity experiments. We have observed an increase of the magnetic entropy change when the material is cooled down to 10–30 K, below which  $-\Delta S_m$  reaches a maximum at 2–3 K, suggesting this to be the starting temperature for an adiabatic demagnetization process. This temperature range is of considerable technological interest because it is easily reachable by pumping liquid helium-4.

## Acknowledgements

This work has been partially supported by Spanish MINECO through grant MAT2009-13977-C03 and by the EPSRC and The Leverhulme Trust (UK).

## References

- [1] For recent overviews, see, (a) M. Evangelisti, E. K. Brechin, *Dalton Trans.* 39 (2010) 4672, and references therein;
- (b) R. Sessoli, *Angew. Chem. Int.-Ed.* 51 (2012) 43, and references therein.
- [2] (a) C. Zimm, A. Jastrab, A. Sternberg, V. K. Pecharsky, K. A. Gschneidner Jr., M. Osborne, I. Anderson, *Adv. Cryog. Eng.* 43 (1998) 1759;
- (b) V. K. Pecharsky, K. A. Gschneidner Jr., *J. Magn. Magn. Mater.* 200 (1999) 44;
- (c) K. A. Gschneidner Jr., A. O. Pecharsky, V. K. Pecharsky, in R. S. Ross Jr. (Ed.), *Cryocoolers 11*, Kluwer Academic/Plenum Press, New York, 2001.
- [3] (a) P. Debye, *Ann. Phys.* 81 (1926) 1154;
- (b) W. F. Giaque, *J. Am. Chem. Soc.* 49 (1927) 1864.
- [4] M.-J. Martínez-Pérez, O. Montero, M. Evangelisti, F. Luis, J. Sesé, S. Cardona-Serra, E. Coronado, *Adv. Mater.* (2012), DOI: 10.1002/adma.201200750.
- [5] Yu. I. Spichkin, A. K. Zvezdin, S. P. Gubin, A. S. Mischenko, A. M. Tishin, *J. Phys. D: Appl. Phys.* 34 (2001) 1162.
- [6] M. Evangelisti, A. Candini, A. Ghirri, M. Affronte, E. K. Brechin, E. J. L. McInnes, *Appl. Phys. Lett.* 87 (2005) 072504.

- [7] M. Manoli, R. D. L. Johnstone, S. Parsons, M. Murrie, M. Affronte, M. Evangelisti, E. K. Brechin, *Angew. Chem. Int.-Ed.* 46 (2007) 4456.
- [8] G. W. Powell, H. N. Lancashire, E. K. Brechin, D. Collison, S. L. Heath, T. Mallah, W. Wernsdorfer, *Angew. Chem. Int.-Ed.* 43 (2004) 5772.
- [9] M. Evangelisti, A. Candini, A. Ghirri, M. Affronte, G. W. Powell, I. A. Gass, P. A. Wood, S. Parsons, E. K. Brechin, D. Collison, S. L. Heath, *Phys. Rev. Lett.* 97 (2006) 167202.
- [10] I. A. Gass, C. J. Milios, M. Evangelisti, S. L. Heath, D. Collison, S. Parsons, E. K. Brechin, *Polyhedron* 26 (2007) 1835.
- [11] C. Vecchini, D. H. Ryan, L. M. D. Cranswick, M. Evangelisti, W. Kockelmann, P. G. Radaelli, A. Candini, M. Affronte, I. A. Gass, E. K. Brechin, O. Moze, *Phys. Rev. B* 77 (2008) 224403.
- [12] See, e.g., M. Evangelisti, F. Luis, L. J. de Jongh, M. Affronte, *J. Mater. Chem.* 16 (2006) 2534.
- [13] (a) G. Karotsis, M. Evangelisti, S. J. Dalgarno, E. K. Brechin, *Angew. Chem. Int. Ed.* 48 (2009) 9928;
- (b) G. Karotsis, S. Kennedy, S. J. Teat, C. M. Beavers, D. A. Fowler, J. J. Morales, M. Evangelisti, S. J. Dalgarno, E. K. Brechin, *J. Am. Chem. Soc.* 132 (2010) 12983;
- (c) J. B. Peng, Q. C. Zhang, X. J. Kong, Y. P. Ren, L. S. Long, R. B. Huang, L. S. Zheng, Z. P. Zheng, *Angew. Chem. Int. Ed.* 50 (2011) 10649;
- (d) M. Evangelisti, O. Roubeau, E. Palacios, A. Camón, T. N. Hooper, E. K. Brechin, J. J. Alonso, *Angew. Chem. Int. Ed.* 50 (2011) 6606;

- (e) J. W. Sharples, Y. Z. Zheng, F. Tuna, E. J. McInnes, D. Collison, *Chem. Commun.* 47 (2011) 7650;
- (f) Y. Z. Zheng, M. Evangelisti, R. E. P. Winpenny, *Chem. Sci.* 2 (2011) 99;
- (g) S. K. Langley, N. F. Chilton, B. Moubaraki, T. Hooper, E. K. Brechin, M. Evangelisti, K. S. Murray, *Chem. Sci.* 2 (2011) 1166;
- (h) Y. Z. Zheng, M. Evangelisti, R. E. P. Winpenny, *Angew. Chem. Int. Ed.* 50 (2011) 3692;
- (i) A. Hosoi, Y. Yukawa, S. Igarashi, S. J. Teat, O. Roubéau, M. Evangelisti, E. Cremades, E. Ruiz, L. A. Barrios, G. Aromí, *Chem. Eur. J.* 17 (2011) 8264;
- (j) Y. Z. Zheng, M. Evangelisti, F. Tuna, R. E. P. Winpenny, *J. Am. Chem. Soc.* 134 (2012) 1057;
- (k) T. Birk, K. S. Pedersen, C. Aa. Thuesen, T. Weyhermüller, M. Schau-Magnussen, S. Piligkos, H. Weihe, S. Mossin, M. Evangelisti, J. Bendix, *Inorg. Chem.* 51 (2012) 5435.